# Efficient mixing by polymers in microchannels

Teodor Burghelea

# Efficient mixing by polymers in microchannels

**Teodor I. Burghelea**

*Université de Nantes, Nantes Atlantique Universités, CNRS, Laboratoire de Thermocinétique de Nantes, UMR 6607, La Chantrerie, Rue Christian Pauc, B.P. 50609, F-44306 Nantes Cedex 3, France*

## Résumé:

*En raison de leur petite taille, les dispositifs microfluidiques doivent fonctionner à bas nombre de Reynolds, Re, c'est pourquoi les écoulements dans les microcanaux de fluides newtoniens sont généralement laminaires et stationnaires. Pour de nombreuses applications pratiques, leurs performances sont limitées par le mélange peu efficace des fluides dans les dispositifs microfluidiques. Ici, nous montrons qu'un écoulement chaotique peut être généré dans un microcanal au Re arbitrairement faible si une petite quantité de polymères flexibles est ajoutée au liquide de travail. Le régime d'écoulement chaotique est caractérisé par une forte intensité des fluctuations du champ de vitesse et une croissance significative de la résistance à l'écoulement. Le flot chaotique conduit à un mélange très efficace, qui est presque indépendant de la diffusion moléculaire.*

## Abstract:

*Due to their small sizes, microfluidic devices are constrained to operate at low Reynolds number, Re, and therefore microscopic flows of Newtonian fluids are typically laminar and stationary. That impedes mixing in microfluidic devices, which limits their performance for many practical applications. Here, we show that truly chaotic flow can be generated in a smooth microchannel of a uniform width at arbitrarily low Re, if a small amount of flexible polymers is added to the working liquid. The chaotic flow regime is characterized by randomly fluctuating three-dimensional velocity field and significant growth of the flow resistance. The chaotic flow leads to quite efficient mixing, which is almost diffusion independent.*

**Keywords : microchannel, elastic turbulence, efficient mixing, Batchelor regime**

## 1 Introduction

Microscopic flows have been attracting an increasing interest during the past decade due to fast development of micro-fluidics and soft lithography [1]. The use of microfluidic devices has few key practical advantages such as the dramatic reduction of the amount of reagents required for fine chemistry and biochemistry [2] applications, well controlled manipulation and sophisticated experiments on single cells [3, 4, 5] and macromolecules [6].

The microscopic flows are almost universally laminar, steady and characterized by a linear dependence of the flow rate on the driving force. These basic characteristics are determined by low values of the Reynolds number, $\mathrm{Re} = \rho V d / \eta$, which is a general measure of the inertial nonlinearity of the flow [7]. Here, V is the mean flow velocity, d is the diameter of the channel, and ϱ and η are the density and the viscosity of the fluid, respectively. When d is reduced, the flow velocity needed to reach a high enough value of Re in order to excite chaotic or turbulent states increases as $d^{-1}$ and the required driving pressure (at fixed aspect ratio) as $d^{-2}$. Therefore, when channels are only few tens of microns wide, achieving high Re requires impractically high driving pressures. A main consequence of the laminar character of the flow is the inefficient mass transfer across the main flow direction, which occurs mainly due to molecular diffusion. Mixing of viscous fluids by diffusion is slow comparative to the mixing that occurs in a random flow. Even for a moderate size protein, such as bovine serum albumin (with a diffusion coefficient $D \approx 3 \cdot 10^{-7} \mathrm{cm}^2/\mathrm{s}$ in water), the diffusion time $d^2/D$ across a micro channel with a width of 100μm is of the order of 100s. Recently, few techniques have been suggested to generate stirring by a three-dimensional flow in order to increase the mixing efficiency in micro-channel flows. They include application of time-dependent external force fields [8, 9]

and increasing Re to moderately high values in curvilinear three-dimensional channels [10, 11].

An ingenious solution to generate chaotic advection in a microscopic flow was suggested in [12]; it involves a special "herringbone" patterning of a micro-channel wall that enhances a secondary flow normal to the mean flow direction. The continuous stretching and folding of the fluid elements (as they advance downstream) results in exponential separation of initially close fluid particles and efficient mixing. However, the flow was stationary in laboratory frame.
A recent experimental work demonstrates that a small addition of high molecular weight linear polymer to a macroscopic flow of a viscous fluid can lead to very efficient mixing in a regime of elastic turbulence [13, 14]. The elastic turbulence is a recently discovered random hydrodynamic process triggered by the nonlinear elastic stresses contributed to the flow by a minute amount of high molecular weight linear polymer molecules, [14]. The elastic turbulence phenomenon can be observed at arbitrarily small Re numbers provided that the nonlinear elastic contribution to the stress tensor dominates the linear relaxation part. This contribution is quantified by the Weissenberg number, $Wi = \lambda \nabla V$ where $\lambda$ is the characteristic relaxation time of the polymer solution. If the size of the flow channel is reduced to a microscopic scale, the extension of polymer molecules in the flow may become comparable to the size of the setup. Therefore, the question whether a microscopic flow of a dilute polymer solution can undergo a purely elastic instability and evolve towards random flow states (in a regime of elastic turbulence) can not be answered by a simple analogy with the macroscopic case and needs to be addressed experimentally.

# 2 Experimental setup and methods

The micro-channel devices consist of a silicon elastomer fabricated by the soft lithography technique [7]. The experiments are conducted in a micro channel consisting of 64 smoothly interconnected curvilinear elements, Fig.1 (A) which are couples of half rings with inner and outer radii $R_i$ = 100μm and $R_o$ = 200μm, Fig.1 (B). It has the same aspect ratio as the macroscopic channel used Ref. [13], but its dimensions are reduced by a factor of 30.

Because of the periodic geometry of the micro-channel, it is convenient to use the number of a segment, N, starting from the inlet as a discrete linear coordinate along the channel. The flow in the micro channels was generated and controlled by pressure differences (controlled within 1Pa accuracy) between the inlets and the outlet, Fig. 1 (A). A 80ppm solution of high molecular weight ($M_w$=18 MDa) polyacrylamide dissolved in a 65% sucrose solution has been used as working fluid. The relaxation time of the solution was $\lambda \approx 3s$ . The flow fields have been investigated using micro particle image velocimetry (micro PIV). For this purpose, the microflows have been illuminated by an expanded laser beam and imaged using an epifluorescent microscope equipped with a low depth of focus objective. The efficiency of mixing of two fluid streams in a microchannel has been quantified by adding a small amount of fluorescent compound (FITC labeled dextran) to one of the fluids and the mixing patterns have been visualized using the confocal scanning microscopy technique.

# 3 Results

## 3.1 Random microflows in a regime of Elastic Turbulence

To characterize the transition to random flow and its statistical properties, long time series (spanning about 2000s) of instantaneous velocity fields have been acquired for various Weissenberg numbers covering both laminar and random flow states. Measurements of time averaged profiles of the tangential and radial velocity components across the channel are presented in Fig. 2 for several values of the Weissenberg number. We have estimated the Weissenberg number by $Wi = 2\lambda V_\theta^{\max} / d$ where d is the channel gap and $V_\theta^{\max}$ is the maximal tangential velocity across the microchannel.

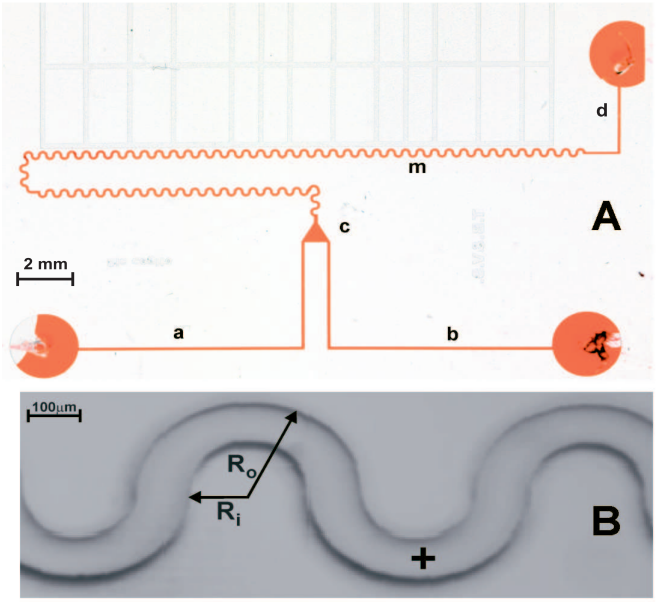


**Figure 1:** (A) Photograph of the microfluidic device. The microchannels were filled with ink for better contrast. (B) Photograph of a section of the functional curvilinear element. The point where instantaneous flow velocity measurements (averaged over a 20X20 µm square region) were made is marked by a cross.

For driving hydrostatic pressures exceeding $\Delta p_s^* = 50Pa\,(Wi^* \approx 13)$, the microflow becomes unstable and a major reorganization of the microflow occurs in the form of a large-scale non-stationary spiral vortex (data not shown here). The Reynolds number corresponding to the onset is $\mathrm{Re}^* \approx 8 \cdot 10^{-5}$. It is worth noting that bellow the transition (squares, circles and triangles in Fig. 2 A), the profiles of the tangential velocity component are clearly non-parabolic and non-symmetric. This difference with respect to the case of a steady and laminar Poiseuille flow in a straight channel has been also observed in experiments with the pure solvent (data not shown here) and agrees rather well with numerical simulations low Re flows in similar geometries. The flow reorganization above the onset of the elastic instability results in an increase in the flow resistance, $\Delta p_s/V$ , Fig. 3(A). As one can see in Fig. 3 (A), the flow resistance is constant in the linear regime corresponding to low values of Wi. Corresponding to $Wi^* \approx 13$, a nonlinear transition occurs and the resistance starts to grow becoming about 1.4 times larger than in the linear regime. This is a first indication of a loss of the hydrodynamic stability of the flow. Time series of the flow velocity have been measured in the middle of the microchannel, which allowed the calculation of both the time averaged velocity and the root mean square (rms) of its fluctuations.

Dependencies of the rms of fluctuations of radial velocity component on Wi are shown in Fig. 3(B). The fluctuations are virtually absent in the linear regime corresponding to low Wi. At $Wi^* \approx 13$, however, both velocity components start to fluctuate and the rms of its fluctuations, $V_{\theta,RMS}$, starts to grow quickly and nonlinearly Fig. 3(B). It can be learned from the inset in Fig. 3(B) that the time -averaged tangential velocity, $V_\theta$, increases linearly at low driving pressures $\Delta p_s$, but its growth slows down at the same critical value of the driving pressure, $\Delta p_s^* = 50Pa\,(Wi^* \approx 13)$, which is further evidence for a nonlinear elastic flow transition taking place.

To conclude this subsection, we show that corresponding to $Wi^* \approx 13$, the flow exhibits a transition to chaotic states. Although the limited resolution of a microscopic flow investigation did not allow us to explore properties of the flow fields down to sufficiently small spatial scales, most of the typical features of elastic turbulent flows in macro channel (see Refs [13,14]) have been surprisingly recovered in a micro channel: fast growth of flow resistance, sudden increase of velocity fluctuations, chaotic point velocity time series. Above the onset the instability, the flow is dominated by a large-scale randomly fluctuating vortex being rather smooth at small scale. This suggested us that Batchelor regime of mixing can be ideally realized in this micro channel flow. The next section is dedicated to this.

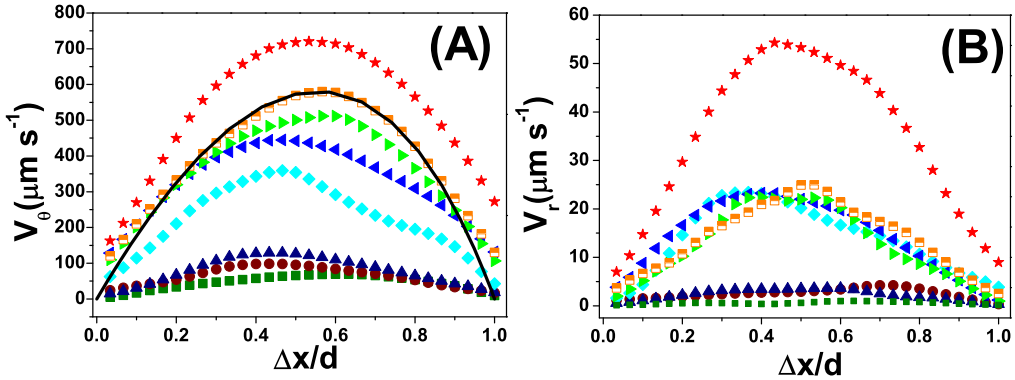


**Figure 2:** Profiles of the (A) tangential velocity component, $V_\theta$ and (B) radial velocity component Vr across the micro-channel. The symbols correspond to: full squares-Wi = 3.84, circles- Wi = 6.75, up triangles-Wi = 8.49, rhumbs-Wi = 13.56, left triangles-Wi = 14.83, right triangles-Wi = 19.4, half filled squares-Wi = 20.15, stars-Wi = 22; the full line is the result of numerical simulations.

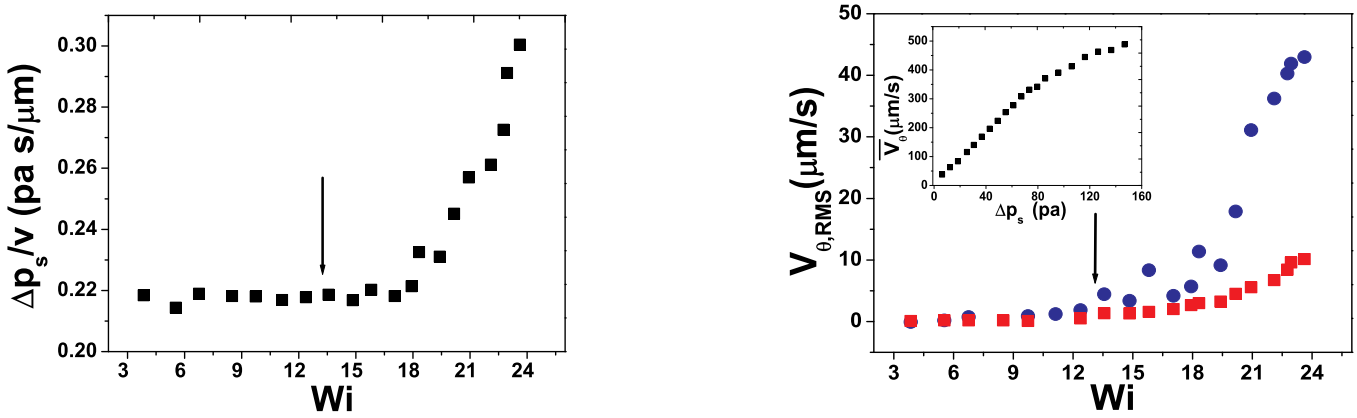


**(A)** **(B)**

**Figure 3: (A)** Flow resistance, $\Delta p_s/V$ vs. Wi. The arrow indicates the onset of the elastic instability. **(B)** Dependence of the rms of fluctuations of the longitudinal component of the flow velocity, $V_{\theta,RMS}$ on Wi, in the center of the micro-channel. The squares are the instrumental error. The arrow indicates the onset of the elastic instability. Inset: Dependence of the time average of the tangential velocity component, $V_\theta$ in the center of the micro-channel on the pressure drop per channel segment, $\Delta p_s$.

## 3.2 Efficient microscopic mixing in a regime of Elastic Turbulence

The question of how efficiently the random flow described in the previous section could mix two viscous fluid streams in a microchannel is addressed in the following. Of particular interest is to understand how the mixing length scales with the Peclet number $Pe = V_{av} d / D$ and to compare with the logarithmic prediction by Batchelor. Here $V_{av}$ stands for the average flow speed and D the molecular diffusion coefficient.

The mixing experiments have been carried out by injecting two streams of polymer solution, one with and one without a fluorescent tracer. The two streams have been injected at equal flow rates by a careful adjustment of the driving pressures (Fig. 4 A).

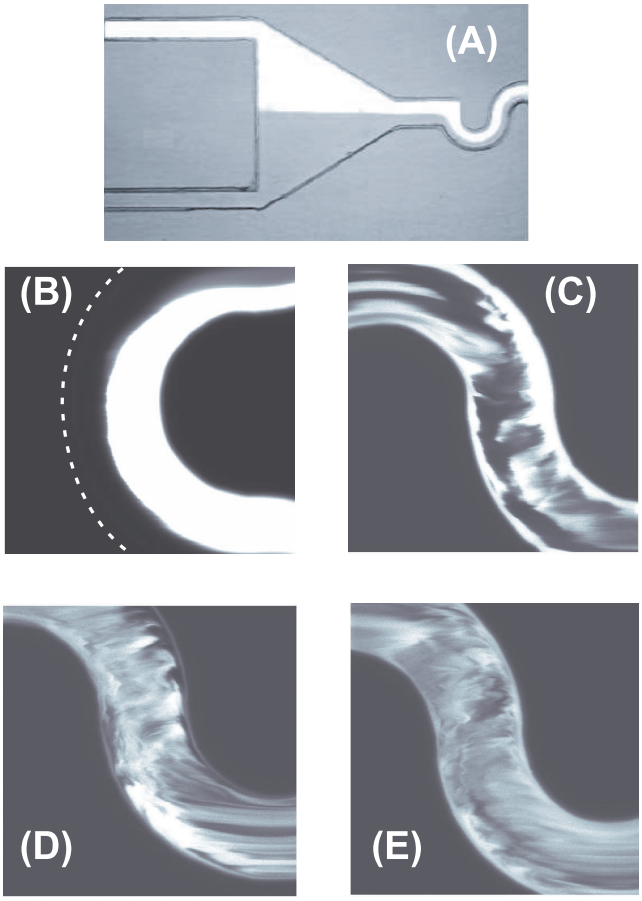


**Figure 4:** **(A)** Epifluorescent microphotograph of the entrance area of a micro-channel. Wide triangular region in front of a curvilinear channel allows one to adjust equal flow rates for polymer solutions with (from the top) and without FITCD. **(B)** Confocal micrograph of the flow in the micro-channel (at N=30) without polymers added. Left wall of the channel is shown by a dotted line. Confocal images of mixing in a random micro flow of a dilute polymer solution at different locations downstream: **(C)** N=5 **(D)** N=11 **(E)** N=17.

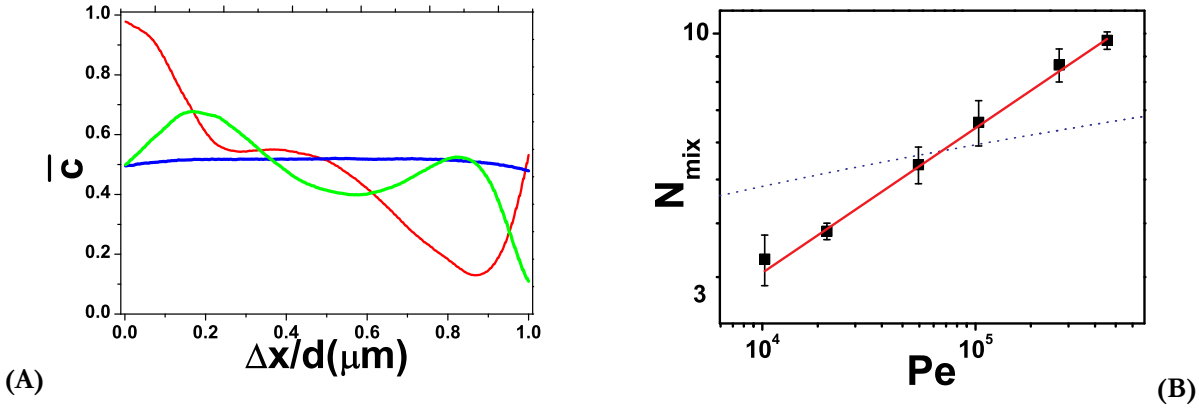


**Figure 5:** **(A)** Time average of FITCD concentration, c, as a function of the normalized coordinate across the micro-channel at different locations downstream: red-N = 7, green- N = 11 and blue-N=41. **(B)** The mixing length, measured in the number of turns, $N_{mix}$, vs. Pe: squares are the data, the solid line is the fit, and the dotted line shows the logarithmic prediction by G. K. Batchelor.

As a passive tracer we have used dextran molecules labelled with fluorescein isothiocyanate (FITCD). The molecular weights of the passive tracers used in the different experiments were 10kDa, 70kDa, 500kDa and 2MDa. These different choices of tracers together with variations of the mean flow velocity allowed us to

modify Pe about 37 times in the range $1.6\times10^4 \div 4.14\times10^5$. First, the setup was tested by running experiments with the plain solvents without polymer added. The flow appeared laminar and steady in the full range of driving pressures, $\Delta p_s$, and the interface between the streams with and without FITCD remained smooth and sharp along the whole channel with only a minor smearing by diffusion Fig. 4 A. The situation was similar when polymer solutions have been injected in the linear regime corresponding to low values of the driving presures, $\Delta$ps. However, when the driving pressure was raised above the nonlinear transition threshold, $\Delta p_s^* = 50Pa\,(Wi^* \approx 13)$, the randomly fluctuating flow velocity produced significant stirring, complex and chaotically changing tracer fields. In Fig. 4 (C-E) are displayed typical scalar fields at different locations downstream. One can easily see that, as one advances downstream, the scalar field has an increasingly random appearance. Corresponding to each value of Pe tested, mixing efficiency has been quantified by focusing on the long time statistics of the concentration distribution across the micro-channel at different positions, N, downstream. Typical time averaged concentration distributions across the micro-channel, c, are displayed in Fig. 5(A). As one advance towards the end of the microchannel (increasing N) the distribution of the passive scalar across the microchannel becomes increasingly homogeneous, indicating a very good mixing. Measurements of the mixing length as a function of Pe are presented in Fig. 5(B). A clear deviation for from the logarithmic prediction by Batchelor is observed in the form of an algebraic scaling of the mixing length. This can be explained by the finite size of the micromixer and the proximity of a mixing boundary layer.

## 4 Conclusions

A detailed experimental study of random microscopic flows of a dilute polymer solution has been presented. Quite remarkably, the nonlinear elastic stresses due to the minute amount of polymer molecules to flow can destabilize the flow at arbitrarily small Reynolds numbers. Several signatures of a turbulent like flow have been captured: flow resistance, a dramatic increase of the velocity fluctuations. It is further shown that the random mircroscopic flow in a regime of Elastic Turbulence can lead to very efficient mixing of two fluid streams. A comparison with the prediction by Batchelor for the evolution of the mixing length with the Peclet number was presented.

## References

[1] G. M. Whitesides, A. D. Stroock, Phys. Today 54 (6), 42 (2001).
[2] C. L. Hansen, E. Skordalakes, J. M. Berger and S. R. Quaqe, Proc. Natl. Acad. Sci. USA 99, 16531 (2002).
[3] N. L. Jeon, H. Baskaran, S. K. W. Dertinger, G. M. Whitesides, L. Van der Wate and M. Toner, Nat. Biotechnol. 20, 826 (2002).
[4] S. Takayama, E. Ostuni, P. LeDuc, K. Naruse, D. E. Ingber, and G. M. Whitesides, Nature (London) 411, 1016 (2001).
[5] H. B. Mao, P. S. Cremer and M. D. Manson, Proc. Natl. Acad. Sci. U.S.A. 100, 5449 (2003).
[6] H. P. Chou, C. Spencer, A. Scherer and S. Quake, Proc. Natl. Acad. Sci. U.S.A. 96, 11 (1999).
[7] Y. N. Xia and G. M. Whitesides, Annu. Rev. Mater. Sci. 28, 153 (1998).
[8] M. H. Oddy, J. G. Santiago, and J. C. Mikkelsen., Anal. Chem. 73, 5822 (2001).
[9] J. H. Tsai and L. W. Lin, Sens. Actuators, A 97, 665 (2000).
[10] D. Therriault, S. R. White, and J. A. Lewis, Nat. Mater. 2, 265 (2003).
[11] R. A. Vijayendran, K. M. Motsegood, D. J. Beebe, and D. E. Leckband, Langmuir,19, 1824 (2003).
[12] A. D. Stroock, S. K. Dertinger, A. Ajdari, I. Mezic, H. A. Stone, and G. M. Whitesides, Science 295, 647 (2002).
[13] A. Groisman and V. Steinberg, Nature (London), 410 (2001) 905.
[14] A. Groisman and V. Steinberg, Nature(London), 405 (2000) 53.